Intention Recognition from Spatio-Temporal Representation of EEG Signals

Lin Yue[1], Dongyuan Tian[2], Jing Jiang[3], Lina Yao[4], Weitong Chen[5], and Xiaowei Zhao[1(✉)]

[1] Northeast Normal University, Changchun, China
zhaoxw303@nenu.edu.cn
[2] Jilin University, Changchun, China
[3] The University of Technology Sydney, Sydney, Australia
[4] University of New South Wales, Sydney, Australia
[5] The University of Queensland, Brisbane, Australia

Abstract. The motor imagery brain-computer interface uses the human brain intention to achieve better control. The main technical problems are feature representation and classification of signal features for specific thinking activities. Inspired by the structure and function of the human brain, we construct a neural computing model to explore the critical issues in the representation and real-time recognition of the state of specific thinking activities. In consideration of the physiological structure and the information processing process of the brain, we construct a multi-scale cascaded Conv-GRU model and extract high-resolution feature information from the dual spatio-temporal dimension, effectively removing signal noise, improving the signal-to-noise ratio, and reducing information loss. Extensive experiments demonstrate that our model has a low dependence on training data size and outperforms state-of-the-art multi-intention recognition methods.

Keywords: Brain-computer interface · Motor imagery · Electroencephalography · Intention recognition

1 Introduction

Brain-computer interface (BCI) can convert neuron activities into signals, thus providing the possibility for discovering the correlation between brain activities and human behaviors. The electroencephalography (EEG) collected by BCI records brain activities with electrophysiological indicators. During brain activity, the sum of postsynaptic potentials is generated synchronously by a large number of neurons. This process records the electrical wave changes during brain activity, reflecting the electrophysiological activities of brain nerve cells in the cerebral cortex or on scalp surface. By analyzing and modeling EEG signals, such models could be applied to clinical practice such as EEG signal-controlled

M. Qiao et al. (Eds.): ADC 2021, LNCS 12610, pp. 1–12, 2021.
https://doi.org/10.1007/978-3-030-69377-0_1

wheelchairs [8], brain wavelet-controlled exoskeleton [9], brain-controlled hearing aid [10], biomedical implant antennas [1], and motor function recovery during rehabilitation [6]. Other application fields include smart living [27], and speech synthesis [3], etc. Through BCI technology, external devices can read brain nerve signals and convert thinking activities into command signals to realize the human mind control. As a result, EEG based intention recognition has been widely studied in recent years and has become one of the most important research topics in pattern recognition.

1.1 Motivation

In EEG signal analysis, the EEG signal segment includes different frequency bands, each with different degrees of correlation with specific brain activity. Specifically, the frequency band represents brain state and qualitative assessment of awareness; the whole band is between 0.5 Hz to 28 Hz [12]. This interval signal can be decomposed into six types of waves, i.e., Delta, Theta, Alpha, Beta1, Beta2, and Beta3. These waves record the characteristics of the motor or sensory nerve action potentials. Among them, the Alpha wave fluctuates in the state of eyes closed and relaxation, while the Beta wave is closely related to motion behavior and attenuation of motion [24]. Different noise levels distribute in these frequency bands, requiring to be removed via adequate measures. Using and separating multiple waves can help to capture correlations between waves and significant features [13,15,16]. On the other hand, extracting the correlations of temporal and spatial features in all signal bands will improve the performance of intention recognition [25]. On this basis, data flow visualization can help to better understand the whole process of brain activity [4]. However, the factors mentioned above have not been fully taken into account when performing motion intention recognition.

1.2 Challenges

EEG based intention recognition developed rapidly and achieved specific gratifying results. Nevertheless, due to technical limitations, there are still some challenges:

- The brain signals are easily disrupted by a variety of biological signals and environmental artifacts.
- Due to the non-stationary characteristics of electrophysiological brain signals, the raw EEG signals have a low signal-to-noise ratio (SNR).
- Existing machine learning studies focus on static data, so it is impossible to classify rapidly changing brain signals accurately.

1.3 Solution

To overcome these challenges, we take temporal features in multivariate time series and spatial information into our consideration during feature representation and develop a model for multi-intention recognition (Fig. 1). To be more

specific, we decompose mixed EEG signal collected with each electrode into signals at frequency bands to reduce noise caused by other frequency ranges and slice the signal series of multiple electrodes into matrices with a sliding window. For filtered EEG arrays, the image mapping layer is utilized for processing EEG arrays into visual images. Finally, we propose multi-scale cascaded Conv-GRU networks (MCG) for image learning with spatio-temporal information. The architecture of the neural network consists of another two parts, i.e., cascaded CNN (convolutional neural network) and GRU (gated recurrent unit), which are used to learn spatio-temporal characteristics, respectively. The multi-intention recognition of dynamic data streams can be effectively solved in this way.

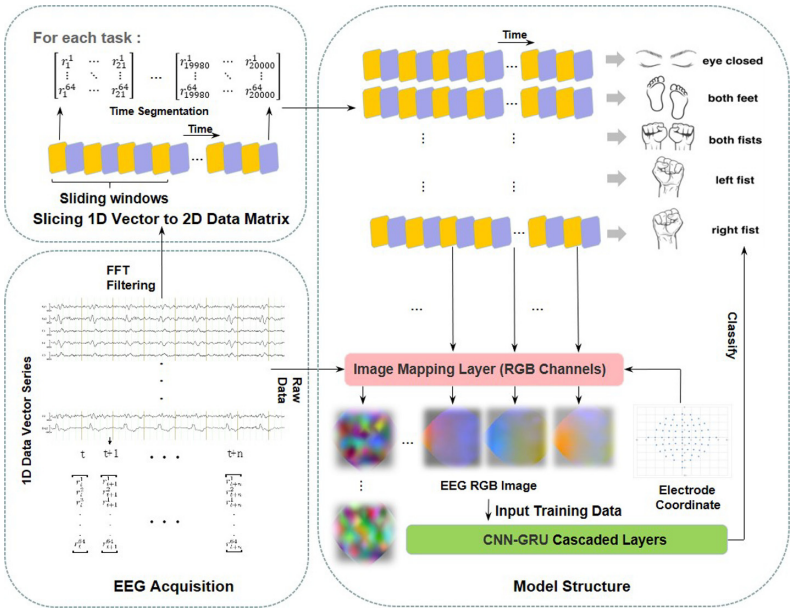

Fig. 1. The workflow of the proposed model MCG.

2 Related Work

Intention recognition can be treated as a classification problem, predicting multiple and subjective human intentions based on EEG traces, rather than actions triggered by events or environment.

Deep learning has been successfully applied in many recognition tasks corresponding to various types of data such as image, video, speech, and text [11,20]. These methods can also be migrated to the task of EEG signal detection. For example, Alomari et al. [2] use a wireless EEG headset as a remote control for a personal computer's mouse cursor. Moreover, in their method, SVM is used for a binary classification task. Kim et al. [13] obtain the Mu and Beta rhythms

from the nonlinear EEG signals and perform prediction using a random forest classifier. Zhang et al. [26] apply deep recurrent neural networks on EEG data and improve performance in multiple classification tasks. At present, the classic solution and EEG state recognition technology are respectively used to select features of continuous-time series and distinguish manifolds between learning states through supervised learning [14]. In BCI systems, processing dynamic data flows often require feature representation with spatio-temporal clues. Modeling the correlations between EEG wavelets and multiple intentions and the problem of multi-intention recognition on dynamical data streams are not well solved yet.

A lot of research has adopted CNN for classification on single-channel EEG [21,23]. At the same time, the feature mapping needs to communicate the complexity of the information without losing original richness or depth. Many successful cases apply ConvNets (convolutional neural networks) to distinguish pathological records from normal EEG recordings in the Temple University Hospital EEG Abnormal Corpus. Furthermore, visualization of the ConvNet decoding behavior shows that they use spectral power changes in Delta (0–4 Hz) and Theta (4–8 Hz) frequency ranges [17]. Similar work has been performed based on deep ConvNets to improve decoding errors in EEG signals of human observers [5]. Among the visual researches of high-dimensional EEG data, many methods visualize data as snapshots or sequential images showing the changing trend by time-lapse method [4]. However, most of the mapping methods in these work use more types of waves, which, to a certain extent, increase the complexity of the method and waste more resources.

3 Method

This section will describe the proposed model multi-scale cascaded Conv-GRU in detail, which is further divided into three parts: data acquisition, image mapping layer, and architecture of neural network.

3.1 Data Acquisition

The EEG signals in this paper are based on the BCI system and collected with a 64/14 electrodes headset. The design of data pretreatment is based on the EEG source data. Specifically, once the subject's action command is given, the 64/14 electrodes will pick up brain signals that reflect the brain activities of different areas. Once a subject generates an intention in mind, the electrodes will pick up voltage fluctuations that reflect multiple brain activities. The voltage values from the scalp will be continuously captured by 64-channel or 14-channel electrode sensors. EEG reading can be represented with a n-dimensional vector $R_t = [r_t^1, r_t^2, ..., r_t^n]$, where the r_t^i is the reading of ith electrode sensor at time step t, it can be seen as 1D vector with a certain amount of noise.

It is commonly known that EEG signals can also be divided into multiple data streams according to frequency ranges, with each band having biological

significance [9,22]. The EEG signals consist of multiple time series corresponding to the measurements at different frequency bands [7]. The EEG signal can be quantified in the frequency range from 0.5 Hz to 28 Hz [5]. The raw EEG signal in r_t^i can be segmented into different categories of bandwidth c, where $c = (\delta, \theta, \alpha, \beta)$. This study focuses on two frequency bands from 8 Hz to 28 Hz, i.e., α and β.

Next, we will define the sliding window that further divides the filtered data. To begins with, we need to ensure the maximum value of the possible window scale. As the data in the EEGMMIDB dataset was collected from 64 electrodes, the sliding window dimension is set as [64, 1] with sliding step size 1 here. The data slices are generated along the time axis, and the resulting data matrix is named a sliding matrix here. Finally, we can get N matrices with spatio-temporal characteristics from the raw data in this way. The data segment is created as follows:

$$S = [s_t, s_{t+1}, ..., s_{t+N-1}] \tag{1}$$

$$s_t = \begin{bmatrix} r_t^1 \\ r_t^2 \\ \vdots \\ r_t^{64} \end{bmatrix} \approx \begin{bmatrix} r_t^{\alpha,1} & r_t^{\beta,1} & r_t^{raw,1} \\ r_t^{\alpha,2} & r_t^{\beta,2} & r_t^{raw,2} \\ \vdots & \vdots & \vdots \\ r_t^{\alpha,64} & r_t^{\beta,64} & r_t^{raw,64} \end{bmatrix} \tag{2}$$

where S_j is the jth data segment at time step $t + j - 1$, $\forall j \in [1...N]$; each electrode r_t^i corresponds to three readings (say $[r_t^{\alpha,i}, r_t^{\beta,i}, r_t^{raw,i}]$) at time t, as the filtering operation is adopted.

3.2 Image Mapping Layer

We convert the spatial distribution of electrodes in three-dimensional space into coordinates in two-dimensional space while preserving the relative distance between adjacent electrodes, as shown in Fig. 2. Specifically, this two-dimensional space is a 32×32 mesh, where each pixel in the mesh is superimposed by three channels, and each channel corresponds to a selected frequency band [4]. In this paper, we select α, β, and raw data as the input of three channels. The next step is the normalization that constrains the data range in a closed interval $[0, 255]$. The image synthesizer combines regularized data and generates suitable pixel values for each targeting coordinate. As different electrodes represent different brain regions, the real-time viewer can capture dynamic results in real-time. The width and height of the energy map represent the spatial distribution of mind activities in the cerebral cortex, and the energy map sequence represents the temporal distribution of mind activities. The energy map sequence (image sequence) $NRGMapSeq$ can be denoted as follows:

$$NRGMapSeq = [I_t, I_{t+1}, ..., I_{t+N-1}] \tag{3}$$

where $NRGMapSeq_j$ is the jth energy map (image) at time step $t + j - 1$, $\forall j \in [1...N]$.

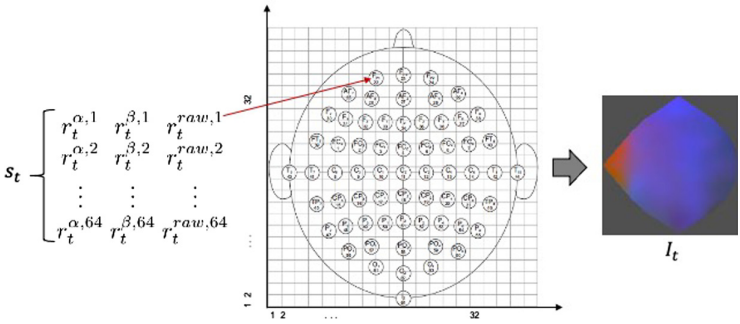

Fig. 2. The process of EEG data segment to image.

3.3 Architecture of the Neural Network

The input of the model is the sequence of 3-channel images (energy maps), which represent the spatial-temporal EEG information. Firstly, the cascaded convolutional neural network will catch partial distribution features from the fragments in image sequence. The performance of the model enhances as the number of convolutional cascade layers increase. After that, the GRU will receive a vector of time series processed by the convolutional cascade layer and further optimize time feature learning.

In order to get detailed and sufficient spatial distribution, the input images can be expressed as:

$$NRGMapSeq = [I_t, I_{t+1}...I_{t+N-1}] \in \mathbb{R}^{N\times c\times h\times w} \tag{4}$$

where N denotes the number of energy maps (images) and the size of each energy map (image) is $c \times h \times w$ (3 channels, height of 32 pixels, width of 32 pixels).

The energy map (image) sequence is input into a Conv2D (two-dimensional convolutional neural networks), and each of the spatial features extracted from the cascaded Conv2D representation is shown in Eq. (5).

$$SP = C_{conv2D}(NRGMapSeq) \tag{5}$$

After the cascaded Conv2D layer, a fully connected layer is applied to connect cascaded Conv2D with the next GRU layer. The RNN has sufficient ability to process arbitrary sequential inputs by recursively applying a transition function to hidden vector h_t. The activation function of the current hidden state h_t at t time step can be computed as follows:

$$h_t = \begin{cases} 0 & \text{t} = 0 \\ \int(h_{t-1}, x_t) & \text{otherwise} \end{cases} \tag{6}$$

where x_t is the current state input, and h_{t-1} is the previous hidden state. However, RNN has difficulty learning long-term dependency. The components

of the gradient vector will vanish or explode exponentially over a long sequence. As a variant of the LSTM (long short-term memory), the GRU synthesizes the forget gate and input gate into one single update gate. Moreover, there is also a mixture of cellular and hidden states with other modifications. The final model is more straightforward than the standard LSTM model. Both LSTM and GRU can retain important features through various gates to ensure that they will not be lost in long-term propagation. Moreover, the GRU transition equations are defined as follows:

$$\begin{aligned} z_t &= \sigma(W_z \cdot [h_{t-1}, x_t]) \\ r_t &= \sigma(W_r \cdot [h_{t-1}, x_t]) \\ h_t &= (1 - z_t) \times h_{t-1} + z_t \times \tanh(W \cdot [r_t \times h_{t-1}, x_t]) \end{aligned} \tag{7}$$

4 Experiments

4.1 Datasets

To verify the validity of the proposed method, we tested the proposed method and all the benchmarking methods with cross-validation on EEGMMIDB[1] and EMOTIV[2], respectively. The intention recognition is treated as a classification task; that is to say, the proposed method MCG will classify five types of intention for both datasets.

4.2 Benchmarking Methods

We compared the proposed model against various state-of-the-art methods. For the baseline models, we kept the same structures and settings. We fed baselines with different features extracted from the same datasets to evaluate the influence of multi-resolution signals. Moreover, a brief introduction of the benchmarking methods as described below:

- Alomari et al. [2]: A support vector machine-based method is used for binary classification, along with features extracted from multi-resolution EEG signals.
- Shenoy et al. [18]: Regularisation is deployed to improve the robustness and accuracy of CSP estimation in features extracting processing. Fisher linear discriminant is used to perform binary tasks.
- Rashid et al. [16]: Neural network (NN) is utilized to perform EEG signal binary-class tasks after decomposing the raw EEG data to extract significant features.
- Kim et al. [13]: Random forest classifier is used for prediction, in which the Mu and Beta rhythms are obtained from the nonlinear EEG signals.
- Sita et al. [19]: Features are extracted from open source EEG data, and LDA solves multiple classification problems.

[1] https://physionet.org/pn4/eegmmidb/.
[2] https://drive.google.com/drive/folders/0B9MuJb6Xx2PIM0otakxuVHpkWkk.

– Zhang et al. [26]: Deep recurrent neural networks are applied on an open EEG database for multiple classifications.
– Chen et al. [7]: Multi-task RNNs model (MTLEEG) is proposed for motion intention recognition based EEG signals.

4.3 Results and Discussion

Visual Verification and Analysis. The image mapping layer generates the brain energy maps, in which each image represents the spatial distribution of the corresponding areas for mind activities, and the energy map sequence represents the temporal distribution or dynamic real-time results. From Fig. 3(a), we can intuitively observe the energy changes corresponding to different actions on different imagery tasks. As displayed in Fig. 3(b), we reserved two brain energy mapping channel respectively. In this way, we can clearly understand the spatio-temporal characteristics of both the two waveforms, which provides more possibilities and ideas for brain working mechanism research.

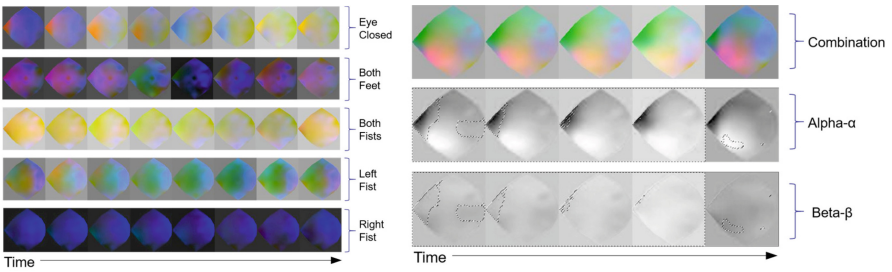

(a) Filtered EEG (Channel 1: α; Channel 2: β; Channel 3: Raw)

(b) Decomposition of waveforms. (Channel 1: α; Channel 2: β; Channel 3: -)

Fig. 3. Brain energy maps from the image mapping layer on EEGMMIDB dataset.

Table 1. Comparisons of different waveband components on EEGMMIDB.

Method	Accuracy	Precision	Recall	F1-score	AUC
MCG-α	0.7722	0.8763	0.7121	0.7857	0.9500
MCG-β	0.8923	0.7707	0.8144	0.7919	0.9619
MCG-α, β	0.9650	0.9650	**0.9806**	0.9727	0.9740
MCG	**0.9870**	**0.9981**	0.9681	**0.9829**	**0.9740**

Effect of Filtering. In this subsection, we used different combinations of waveforms to test the model in terms of accuracy, precision, recall, F1-score, and AUC. As shown in Table 1, for the combination of input signal (α, β, raw), MCG achieves the best performance on multiple indicators on the whole, which directly verifies the importance of filtering and the combination of raw signal

Table 2. Comparisons of evolution models on EEGMMIDB.

Input	Method	Class	Accuracy
α	CNN	Multiple (5)	0.7109
α	CasCNN	Multiple (5)	0.7556
α	CasCNN+GRU	Multiple (5)	**0.7722**
β	CNN	Multiple (5)	0.7161
β	CasCNN	Multiple (5)	0.7632
β	CasCNN+GRU	Multiple (5)	**0.8923**
α, β	CNN	Multiple (5)	0.8218
α, β	CasCNN	Multiple (5)	0.7723
α, β	CasCNN+GRU	Multiple (5)	**0.9829**
α, β, raw	CNN	Multiple (5)	0.8401
α, β, raw	CasCNN	Multiple (5)	0.9356
α, β, raw	**CasCNN+GRU**	Multiple (5)	**0.9868**

with α and β. This combination maximally preserves the useful wavebands and avoids the loss of the original features of the data.

Comparisons of Evolution Models. Furthermore, we compared MCG with evolution models of CNN and cascade structure CNN (see Table 2). In the scope of this paper, the evolution model means we remove some layers in the model, such as GRU and CasCNN, and only use the deep convolutional network (CNN) to train the data. By observing the influence of these layers on the experimental results, we could see that both GRU and CasCNN improved the accuracy.

Comparisons of MCG and Benchmarking Methods. To prove the generalization and robustness of MCG, we further compared MCG with multiple state-of-the-art methods, on EEGMMIDB and EMOTIV datasets. Although the EMOTIV is collected with EMOTIV Epoc+ headset, which contains fewer sensors and has a lower sampling rate, i.e., 14 sensors and 128 Hz sampling rate. The comparisons as shown in Table 3 and 4, have vividly illustrated that MCG achieve stable and brilliant performance in terms of accuracy.

Table 3. Comparisons of MCG and benchmarking methods on EEGMMIDB.

Index	Method	Class	Accuracy
1	Almoari et al. [2]	Binary	0.7500
2	Shenoy et al. [18]	Binary	0.8206
3	Rashid et al. [16]	Binary	0.9199
4	Kim et al. [13]	Multiple (3)	0.8050
5	Sita et al. [19]	Multiple (3)	0.8500
6	Zhang et al. [26]	Multiple (5)	0.9590
7	Chen et al. [7]	Multiple (5)	0.9786
8	**MCG**	Multiple (5)	**0.9868**

Table 4. Comparisons of MCG and benchmarking methods on EMOTIV.

Index	Method	Class	Accuracy
1	Almoari et al. [2]	Binary	0.5627
2	Shenoy et al. [18]	Binary	0.5553
3	Rashid et al. [16]	Binary	0.7538
4	Kim et al. [13]	Multiple (3)	0.7695
5	Sita et al. [19]	Multiple (3)	0.6985
6	Zhang et al. [26]	Multiple (5)	0.7361
7	Chen et al. [7]	Multiple (5)	0.8396
8	**MCG**	Multiple (5)	**0.8600**

5 Conclusions

In this paper, we propose MCG model, which uses the image mapping layer to capture spatial information of the EEG signals and combines spatial-temporal characteristics to identify multiple motion intentions. The proposed model is capable of discovering the brain changes corresponding to different actions. That is, the feature representation achieved through the image mapping layer reflects not only the changes in brain-related different movements but also dynamic responses of the brain in real-time corresponding to specific actions. Experimental results illustrate that the recognition efficiency is the highest among state-of-the-are methods on the multi-classification task of intention recognition.

Acknowledgement. This research has been supported by the Fundamental Research Funds for the Central Universities under Grant No. 2412019FZ047, the China Postdoctoral Science Foundation under Grant No. 2017M621192, the National Natural Science Foundation of China (NSFC) under Grant No.61972384, and the Outstanding Sino-foreign Youth Exchange Program of China Association for Science and Technology.

References

1. Agarwal, K., Guo, Y.X.: Interaction of electromagnetic waves with humans in wearable and biomedical implant antennas. In: 2015 Asia-Pacific Symposium on Electromagnetic Compatibility (APEMC), pp. 154–157. IEEE (2015)
2. Alomari, M.H., AbuBaker, A., Turani, A., Baniyounes, A.M., Manasreh, A.: EEG mouse: a machine learning-based brain computer interface. Int. J. Adv. Comput. Sci. Appl. **5**(4), 193–198 (2014)
3. Anumanchipalli, G.K., Chartier, J., Chang, E.F.: Speech synthesis from neural decoding of spoken sentences. Nature **568**(7753), 493 (2019)
4. Bashivan, P., Rish, I., Yeasin, M., Codella, N.: Learning representations from EEG with deep recurrent-convolutional neural networks. arXiv preprint arXiv:1511.06448 (2015)

5. Behncke, J., Schirrmeister, R.T., Burgard, W., Ball, T.: The signature of robot action success in EEG signals of a human observer: Decoding and visualization using deep convolutional neural networks. In: 2018 6th International Conference on Brain-Computer Interface (BCI), pp. 1–6. IEEE (2018)
6. Biryukova, E., et al.: Arm motor function recovery during rehabilitation with the use of hand exoskeleton controlled by brain-computer interface: a patient with severe brain damage. Fiziol. Cheloveka **42**(1), 19–30 (2016)
7. Chen, W., et al.: EEG-based motion intention recognition via multi-task RNNs. In: Proceedings of the 2018 SIAM International Conference on Data Mining, pp. 279–287. SIAM (2018)
8. Fiala, P., Hanzelka, M., Čáp, M.: Electromagnetic waves and mental synchronization of humans in a large crowd. In: 2017 11th International Conference on Measurement, pp. 241–244. IEEE (2017)
9. Frolov, A.A., Húsek, D., Biryukova, E.V., Bobrov, P.D., Mokienko, O.A., Alexandrov, A.: Principles of motor recovery in post-stroke patients using hand exoskeleton controlled by the brain-computer interface based on motor imagery. Neural Netw. World **27**(1), 107 (2017)
10. Han, C., O'Sullivan, J., Luo, Y., Herrero, J., Mehta, A.D., Mesgarani, N.: Speaker-independent auditory attention decoding without access to clean speech sources. Sci. Adv. **5**(5), eaav6134 (2019)
11. He, K., Zhang, X., Ren, S., Sun, J.: Spatial pyramid pooling in deep convolutional networks for visual recognition. IEEE Trans. Pattern Anal. Mach. Intell. **37**(9), 1904–1916 (2015)
12. Kaiser, A.K., Doppelmayr, M., Iglseder, B.: EEG beta 2 power as surrogate marker for memory impairment: a pilot study. Int. Psychogeriatr. **29**(9), 1515–1523 (2017)
13. Kim, Y., Ryu, J., Kim, K.K., Took, C.C., Mandic, D.P., Park, C.: Motor imagery classification using mu and beta rhythms of EEG with strong uncorrelating transform based complex common spatial patterns. Comput. Intell. Neurosci. **2016**, 1 (2016)
14. Lotte, F., Congedo, M., Lécuyer, A., Lamarche, F., Arnaldi, B.: A review of classification algorithms for EEG-based brain-computer interfaces. J. Neural Eng. **4**(2), R1 (2007)
15. Moore, M.R., Franz, E.A.: Mu rhythm suppression is associated with the classification of emotion in faces. Cogn. Affect. Behav. Neurosci. **17**(1), 224–234 (2016). https://doi.org/10.3758/s13415-016-0476-6
16. or Rashid, M.M., Ahmad, M.: Classification of motor imagery hands movement using Levenberg-Marquardt algorithm based on statistical features of EEG signal. In: 2016 3rd International Conference on Electrical Engineering and Information Communication Technology (ICEEICT), pp. 1–6. IEEE (2016)
17. Schirrmeister, R.T., et al.: Deep learning with convolutional neural networks for EEG decoding and visualization. Hum. Brain Mapp. **38**(11), 5391–5420 (2017)
18. Shenoy, H.V., Vinod, A.P., Guan, C.: Shrinkage estimator based regularization for EEG motor imagery classification. In: 2015 10th International Conference on Information, Communications and Signal Processing (ICICS), pp. 1–5. IEEE (2015)
19. Sita, J., Nair, G.: Feature extraction and classification of EEG signals for mapping motor area of the brain. In: 2013 International Conference on Control Communication and Computing (ICCC), pp. 463–468. IEEE (2013)
20. Song, S., Miao, Z.: Research on vehicle type classification based on spatial pyramid representation and BP neural network. In: Zhang, Y.-J. (ed.) ICIG 2015. LNCS, vol. 9219, pp. 188–196. Springer, Cham (2015). https://doi.org/10.1007/978-3-319-21969-1_17

21. Sors, A., Bonnet, S., Mirek, S., Vercueil, L., Payen, J.F.: A convolutional neural network for sleep stage scoring from raw single-channel EEG. Biomed. Signal Process. Control **42**, 107–114 (2018)
22. Tatum, W.O.: Ellen R. grass lecture: extraordinary EEG. Neurodiagnostic J. **54**(1), 3–21 (2014)
23. Tsinalis, O., Matthews, P.M., Guo, Y., Zafeiriou, S.: Automatic sleep stage scoring with single-channel EEG using convolutional neural networks. arXiv preprint arXiv:1610.01683 (2016)
24. Wang, S., Chang, X., Li, X., Long, G., Yao, L., Sheng, Q.Z.: Diagnosis code assignment using sparsity-based disease correlation embedding. IEEE Trans. Knowl. Data Eng. **28**(12), 3191–3202 (2016)
25. Zhang, D., Yao, L., Zhang, X., Wang, S., Chen, W., Boots, R.: EEG-based intention recognition from spatio-temporal representations via cascade and parallel convolutional recurrent neural networks. arXiv preprint arXiv:1708.06578 (2017)
26. Zhang, X., Yao, L., Huang, C., Sheng, Q.Z., Wang, X.: Intent recognition in smart living through deep recurrent neural networks. In: Liu, D., Xie, S., Li, Y., Zhao, D., El-Alfy, E.S. (eds.) ICONIP 2017. LNCS, vol. 10635, pp. 748–758. Springer, Cham (2017). https://doi.org/10.1007/978-3-319-70096-0_76
27. Zhang, X., Yao, L., Sheng, Q.Z., Kanhere, S.S., Gu, T., Zhang, D.: Converting your thoughts to texts: enabling brain typing via deep feature learning of EEG signals. In: 2018 IEEE International Conference on Pervasive Computing and Communications (PerCom), pp. 1–10. IEEE (2018)